Journal of Power Sources 217 (2012) 503–508

Contents lists available at SciVerse ScienceDirect

Journal of Power Sources

journal homepage: www.elsevier.com/locate/jpowsour

Composition analysis of the solid electrolyte interphase film on carbon electrode of lithium-ion battery based on lithium difluoro(oxalate)borate and sulfolane

Shiyou Li, Xiaoli Xu, Xinming Shi, Bucheng Li, Yangyu Zhao, Hongming Zhang, Yongli Li, Wei Zhao, Xiaoling Cui*, Liping Mao

College of Petrochemical Technology, Lanzhou University of Technology, Lanzhou 730050, China

HIGHLIGHTS

- When used in Li/MCMB cells LiODFB–EMC/SL electrolyte exhibit low impedance of SEI film.
- SEI film undergoes a smoothing and destroying process as cycling.
- Compositions of the SEI film in Li/MCMB cell with LiODFB–EMC/SL electrolyte contain at least C_2H_5OLi, $C_2H_5CO_3Li$, Li_2CO_3, RSO_3Li, Li_2SO_3, LiF, C_2H_5F and some complicated mesh compounds based on >B–O– bond.
- Impedance reduction benefits from both the rich existence of sulfurous compounds and the low content of LiF in SEI film.

ARTICLE INFO

Article history:
Received 4 February 2012
Received in revised form
4 May 2012
Accepted 29 May 2012
Available online 9 June 2012

Keywords:
Impedance
Lithium difluoro(oxalate)borate
Solid electrolyte interphase
Sulfolane

ABSTRACT

As a promising salt for lithium-ion batteries, lithium difluoro(oxalate)borate (LiODFB) has become a research hotspot in recently. In this work, LiODFB-based electrolytes are studied. When used in Li/MCMB (mesophase carbon microbeads) cells, cell with 0.9 M LiODFB–ethyl methyl carbonate (EMC)/sulfolane (SL) (1:1, v/v) electrolyte shows lower impedance than ones with 0.9 M LiODFB–EMC/ethylene carbonate (EC) (1:1, v/v) electrolyte. Reduction of impedance mainly dues to the fitting nature of solid electrolyte interphase (SEI) film on carbon electrode of lithium-ion battery. The changing morphologies of SEI films with increased circulation numbers were analyzed by scanning electron microscope (SEM). And C_2H_5OLi, $C_2H_5CO_3Li$, Li_2CO_3, RSO_3Li, Li_2SO_3, LiF, C_2H_5F and some complicated mesh compounds based on >B–O– bond, were found in SEI film by Fourier transform infrared spectroscopy (FTIR) and X-ray photoelectron spectroscopy (XPS). It was believed that the root of impedance reduction benefits from both the rich existence of sulfurous compounds and the low content of LiF in SEI film.

1. Introduction

Carbonaceous materials are widely employed as the anodes in lithium-ion batteries. Much effort has been devoted to the improvement of the reversible performance of these insertion materials [1]. Besides, a passive film named solid electrolyte interphase (SEI) film is found on the surface of the carbon electrode after the charging–discharging processes. This film plays a critical role in the performance of the lithium-ion batteries. It has been found that the carbon material has good cycle life and maintains a high potential due to the formation of a good SEI film on the carbon surface [2,3].

The quality and composition of the SEI mostly depend on the ingredient of the electrolyte which consists of a lithium salt and organic solvents. As a prospecting salt for lithium-ion battery, lithium oxalyldifluoroborate (LiODFB) has been known to strongly facilitate the formation of SEI film on the surface of carbonaceous anode materials [4–8]. Besides, it is of many advantages as follows [9], (1) it is more soluble than other salts in linear carbonate solvents that are essential to lower viscosity and increase wettability of the lithium-ion electrolytes, (2) LiODFB-based electrolyte has excellent film performance even in pure propylene carbonate (PC), and results in a little irreversible capacity at about 2 V in the first cycle of lithium-ion battery due to the lower concentration of the oxalate group in its molecule, and (3) the lithium-ion battery based on LiODFB has good power capability and low-temperature cycle performance.

It was reported that formation of SEI film is not only due to the nature of salt selected in electrolyte system, but also affected by solvents composition [2]. Therefore, exploring of appropriate electrolytes in order to improve the electrochemical

* Corresponding author. Tel.: +86 931 2973305; fax: +86 931 2973648.
E-mail address: xiaoli562@126.com (X. Cui).

0378-7753/$ – see front matter
http://dx.doi.org/10.1016/j.jpowsour.2012.05.114

performance of SEI film for LiODFB-based cell is of special interest.

Alkyl carbonates such as ethylene carbonate (EC), diethyl carbonate (DEC), methyl ethyl carbonate (EMC) and dimethyl carbonate (DMC) are among the most important solvents for electrolytes of lithium-ion batteries because they are aprotic, polar and non-volatile [10]. Sulfolane (SL) is a common solvent known for high dielectric constant, boiling point, flash point, electrochemical stability and solubility, though it has high melting point (27.4–27.8 °C) and high viscosity (10.286 mPa s, at 30 °C). So, in this study, a linear carbonate solvent such as EMC was chosen to realize advanced complementation.

With help of excellent film performance of LiODFB itself, LiODFB–EMC/SL electrolyte has been proved to form a stable SEI film on surface of cathode materials in our prevenient work. In this paper, electrochemical impedance spectroscopy (EIS) two kinds of cells respectively using LiODFB–EMC/SL and LiODFB–EMC/EC electrolyte are compared. And series of tests are used to identify compositions of the SEI film, to explain the film formation process and the beneficial ingredients of solvent systems for advanced lithium-ion batteries.

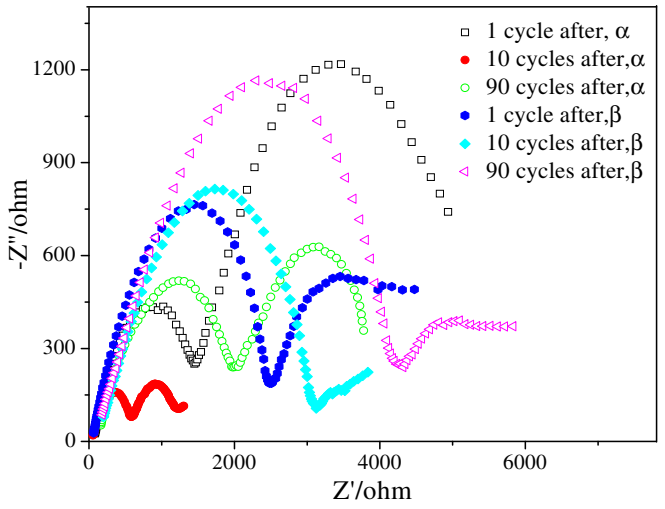

Fig. 1. EIS spectra of cells with 0.9 M LiODFB-EMC/SL (a) and 0.9 M LiODFB–EMC/EC (b) electrolytes after various lithiation processes recorded in 0.003 V at room temperature.

2. Experimental

The negative electrode was composed of 92 wt.% meso-carbon microbeads (MCMB) and 8 wt.% polyvinylidene difluoride (PVDF, as a binder) in *N*-methyl-2-pyrrolidone. Slurry was scrawled on an Al sheet and then dried at 90 °C for 4 h in a vacuum oven to make the negative electrode. Metallic lithium strip was used as both counter and reference electrodes. Celgard PP (poly-propylene) membrane was used as separator. 0.9 M LiODFB–EMC/SL (1:1, v/v, tags for α) or 0.9 M LiODFB–EMC/EC (1:1, v/v, tags for β) was used as electrolyte to assemble Li/MCMB cell in an argon atmosphere glove box, respectively.

EIS spectra of the negative electrode were measured in a three-electrode cell (the negative electrode was used as working electrode with the reaction area of 1 cm^2, and lithium sheet was used both as counter electrode and reference electrode) through CHI660C electrochemical analyzer (Shanghai, China) at 0.003 V. A sinusoidal AC perturbation of 2 mV was applied to the electrode over the frequency range of 100 kHz to 10 mHz.

Electrochemical properties tests of cells were carried out on a land cell tester CT2001A (Wuhan, China) in the voltage range of 0.003–2 V with a constant current density of 0.25 mA cm^{-2} at room temperature.

Negative materials were stripped off from carbon electrodes, washed with dimethyl carbonate (DMC), and dried at 100 °C for 12 h. Prepared samples were characterized by Fourier transform infrared spectroscopy (FTIR) (FTIR-650), scanning electronic microscopy (SEM, JSM-6701F) and X-ray photoelectron spectroscopy (GG314-JPS-9200) measurements, respectively.

3. Results and discussion

3.1. EIS measurement

Fig. 1 shows EIS spectra of cells with α or β electrolyte after various times of complete lithiation processes recorded at 0.003 V at room temperature. The first overlapped semicircle in high frequency range stands for impedance of SEI film. As shown in Fig. 1, for the cell with α electrolyte, impedance of 1 cycle after is a little big. With a continuous modification, a pyknotic and conductive SEI film is formed after 10 cycles to decrease migration resistance of Li^+ ions. Therefore, the impedance becomes very small and the cycle stability of the cell will be improved. After 90 cycles, impedance of SEI film becomes big again, which is caused by the decomposition of SEI film. In the same situation, impedance of the cell with β electrolyte becomes big along with cycles, and is always larger than cell with α electrolyte since 10 cycles after. Results above proved that the cell with α electrolyte owns lower impedance of SEI film which presages a better cycle performance. So, the following study will be focused on α electrolyte.

3.2. SEM measurement

Fig. 2 shows the surface morphologies of negative electrodes of Li/MCMB cells with α electrolyte. It is so roughly that nothing adheres to the surface of sample without cycle (Fig. 2a_1 and a_2). While after 1 cycle, surface of the sample becomes smooth and a loose SEI film is formed (Fig. 2b_1 and b_2). And morphologies show thickness of the sample is 261 μm, while thickness of SEI film is about 23.1–49 nm (Fig. 2c_1). After 10 cycles (Fig. 2d_1 and d_2), the SEI film becomes pyknotic which helps transfer of Li^+ ions. After 90 cycles, evident fissure emerges on the surface of MCMB particles in Fig. 2e_1 and e_2. It implies stability of the SEI film is destroyed, the cycle performance of Li/MCMB cell will be reduced. All of these phenomena accord with results getting from Fig. 1 that impedance of the cell becomes small from 1 cycle to 10 cycles after, and then becomes big from 10 cycles after to 90 cycles after.

3.3. Component analysis

3.3.1. FTIR measurement

Fig. 3 shows the FTIR spectra of samples with α electrolyte before and after cycles, respectively. Characteristic peaks of negative materials on the surface of negative electrodes without cycle nearby 1632.58, 1396.44, 1322.34, 1182.37, 1119.15 and 882.66 cm^{-1} (Fig. 3b), which are similar to peaks of unassembled sample (Fig. 3a) are shown in the spectra. It indicates that, before cycle, no obvious chemical reaction occurs on the surface of MCMB particles without electric current. Except for peaks mentioned above, some other peaks also emerge in curves of Fig. 3c and d. Peaks at 2928.40 ($\upsilon_s CH_2$), 2859.18 ($\upsilon_{as} CH_2$), 1420.85 ($\delta_{as} C–CH_3$),

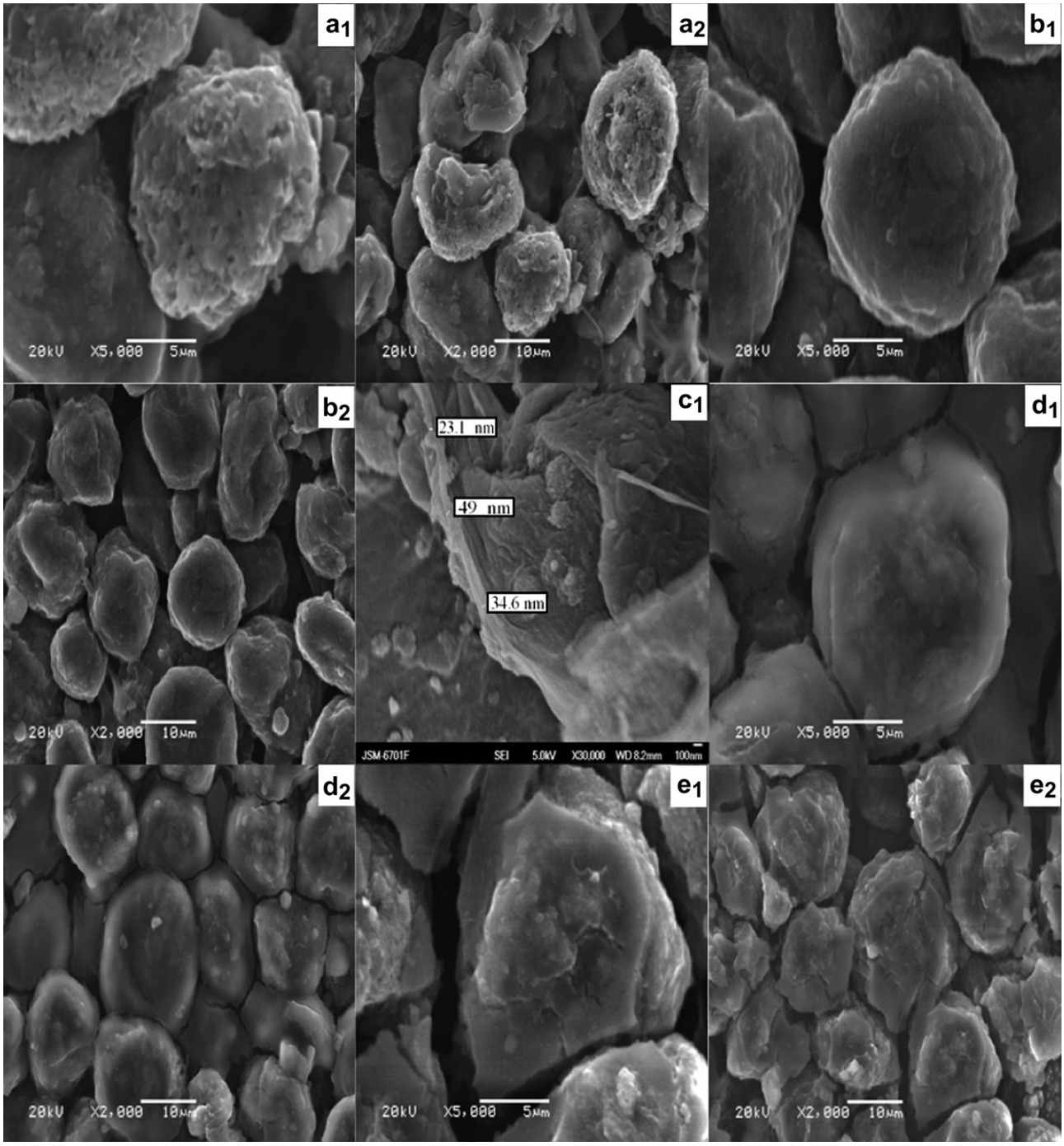

Fig. 2. SEM of graphite cathode: a_1 and a_2, uncycled (magnifying power is 5000 and 2000, respectively, the same as follows); b_1 and b_2, 1 cycle after; c_1, cross section of graphite cathode after 1 cycle (magnifying power is 250); d_1 and d_2, 10 cycles after; e_1 and e_2, 90 cycles after.

2968.01 ($\upsilon_{as}C{-}CH_3$), 2859.18 ($\upsilon_sC{-}CH_3$) and 1100 ($\upsilon C{-}O$) cm^{-1} denote existence of C_2H_5OLi. Peaks at 1639.46 ($\upsilon_{as}COO^-$), 1326.62 (υ_sCOO^-) and 817.69 ($\delta OCOO^-$) cm^{-1} prove existence of $C_2H_5CO_3Li$ [16]. Li_2CO_3 is found with the characteristic peaks at 1420.85 and 817.69 ($\delta OCOO^-$) cm^{-1}. Peak at 775 cm^{-1} demonstrates the existence of LiF. Moreover, some more complicated mesh compounds [4] than that of (1) I and II maybe are formed based on >B–O– (1119.06 cm^{-1}) bond [11]. All of these compounds are imported by the decomposition of EMC and LiODFB. Possible mechanisms are exhibited as follows:

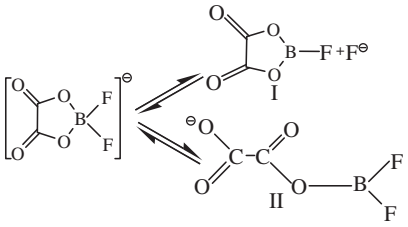

(1)

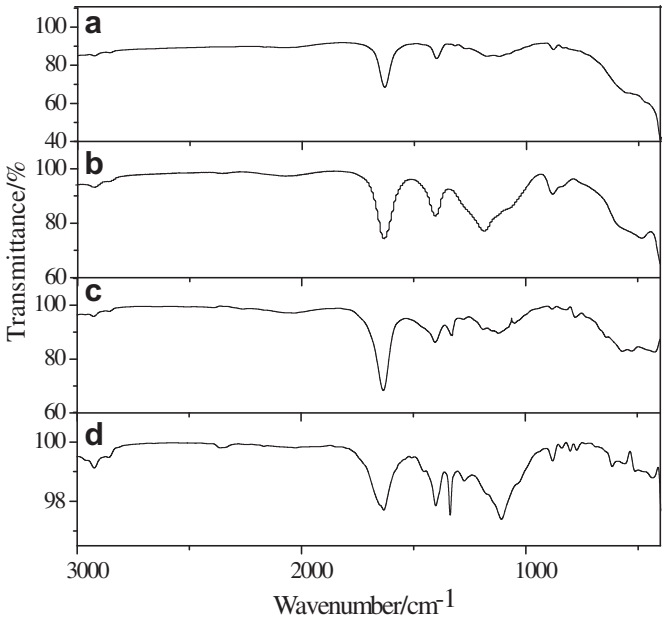

Fig. 3. FTIR spectrum of graphite cathode in Li/MCMB cell with 0.9 M LiODFB–EMC/SL electrolyte for several cycles: (a) unassembled, (b) uncycled, (c) 1 cycle after, (d) 10 cycles after.

$$Li^+ + F^- \rightarrow LiF \quad (2)$$

$$EMC \rightarrow (C_2H_5)_2CO_3\ (DEC) + (CH_3)_2CO_3\ (DMC) \quad (3)$$

$$DEC + e + Li^+ \rightarrow C_2H_5CO_2^{\bullet} + C_2H_5CO_3Li/C_2H_5OLi + C_2H_5^{\bullet} + CO_2 \quad (4)$$

$$C_2H_5^{\bullet} + F^- \rightarrow C_2H_5F + e \quad (5)$$

$$H_2O\ (trace) + 2e + 2Li^+ \rightarrow Li_2O + H_2 \quad (6)$$

$$2Li^+ + e + CO_2 \rightarrow Li_2CO_3 \quad (7)$$

The peak at 1180.75 cm^{-1} proves the existence of RSO_3Li. Peaks at 1180.75 ($\upsilon_{as}SO_3^-M^+$) and 1048.38 ($\upsilon_sSO_3^-M^+$) cm^{-1} are characteristic absorption peaks of Li_2SO_3, which are introduced by the decomposition of SL and LiODFB. The possible mechanism is shown as follows:

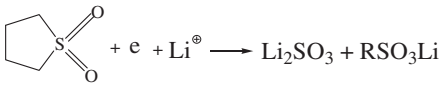

(8)

Possible equation (8) takes place at above 1.5 V, at which potential the equation (1) also takes place [12]. The strong effects between anion and cation of these substances are easily to result in deposition of multilayer film, so that SEI film formed in the beginning can protect negative electrode from being destroyed. Besides, as intensity of these chemical reactions are small, only a few Li^+ ions are consumed, which reduces loss of irreversible capacity of the cell. Despite reduction products of SL and LiODFB retained as a component of the preliminary SEI layer on the MCMB surface, formation of the SEI film is preliminary and unstable, indicating that it only plays a guide role for the follow-up formation of the SEI film (equations (2)–(7)) [12,13].

When Fig. 3d was compared with Fig. 3c, almost all characteristic relative peak areas of C_2H_5OLi, $C_2H_5CO_3Li$, Li_2CO_3, RSO_3Li, Li_2SO_3 and complicated mesh compounds based on >B–O– bond become big after 10 cycles, while the relative peak area of LiF becomes smaller evidently. As LiF is a poor conductor of Li^+ ions, the lower content of LiF helps to impedance reduction [14]. This phenomenon accords well with the result getting from Fig. 1 that the impedance of cell becomes small from 1 cycle to 10 cycles after.

3.3.2. XPS measurement

Fig. 4 shows XPS spectra of samples without cycle and after 1 cycle, respectively. Three peaks emerge at about 284.8, 286.8 and 292.0 eV in C 1s spectrum (Fig. 4a) for the sample without cycle. 284.8 eV is characteristic peak of C 1s of MCMB, the other two peaks at 286.8 and 292.0 eV are C 1s peaks introduced by $(-C^*H_2CF_2-)_n$ and $(-CH_2C^*F_2-)_n$ of PVDF [15]. After 1 cycle (Fig. 4b), peaks nearby 284.4, 284.9, 288.8 and 290.5 eV correspond with C_2H_5OLi, C–C, $C_2H_5CO_3Li$ and Li_2CO_3 [16], respectively. Formations of $C_2H_5CO_3Li$, C_2H_5OLi and Li_2CO_3 make compositions of SEI film link with edge of MCMB in structure, so the SEI film becomes more stable, and intercalation and deintercalation capacity of Li^+ ions in the cathode are also improved. Besides, these compounds can eliminate the carbon chain, carbon-bear free radicals and other heteroatom, increase numbers of nanometer channels and micropores, which are in favor of migrations of Li^+ ions and their storage, respectively.

For sample without cycle, as shown in Fig. 4c, only one peak of C–F appears in F 1s spectra (about 689.3 eV, caused by PVDF). But after 1 cycle, this peak disappears for the surface of negative electrode is covered completely by formation of a SEI film, and leads to two new peaks emerge at 687.4 and 684.9 eV. These peaks are respectively corresponded with LiF and C_2H_5F which are generated from equations (2) and (5).

As shown in Fig. 4d, no peak appears in the B 1s spectrum for the sample without cycle. But after 1 cycle, an obvious peak emerges at 192.3 eV. It denotes existence of complicated mesh compounds based on >B–O– bond. These substances can be combined with reductive products of solvents (RCO_3Li for example), which will improve stability of the SEI film, and provide the SEI film tenacity, uniformity and densification [4,17–19]. As a result, electrochemical properties of anode materials will be greatly improved.

As shown in Fig. 4e, no peak appears in the Li 1s spectrum for the sample without cycle. But after 1 cycle, three peaks obviously emerge at 55.5, 53.8 and 56.4 eV. They are characteristic peaks of $LiOCH_2CH_3$, Li_2O and LiF, respectively. The content of LiF in SEI film is only about 18.36%, lower than that of typical $LiPF_6$-based electrolyte (as high as about 20–40%) [20]. It helps to impedance reduction and electrochemical performance improvement. It is more attractive that content of LiF will become lower along with cycles, as shown in Fig. 3.

As shown in Fig. 4f, only one peak emerges at about 534.2 eV in the O 1s spectrum of the sample without cycle. It may be caused by C–H, C–OH, and C–O– surface groups, which are formed by the reaction between active carbon sites and moist air. After 1 cycle, the peak disappears in surface of negative electrode covering completely after formation of a SEI film. Two new peaks emerge at 531.7 and 528.6 eV, which are respectively corresponded with $LiOC_2H_5$ and Li_2O.

As shown in Fig. 4g, no peak appears in the S 2p spectrum for the sample without cycle. But after 1 cycle, three peaks obviously emerge at 167.9, 168.6 and 169.3 eV, which are characteristic peaks of RSO_3Li, Li_2SO_3 and Li_2SO_4, respectively. Both of RSO_3Li and Li_2SO_3 are observed through equation (8), and Li_2SO_4 maybe resulted from oxidation of Li_2SO_3 during the process of preparation or analysis.

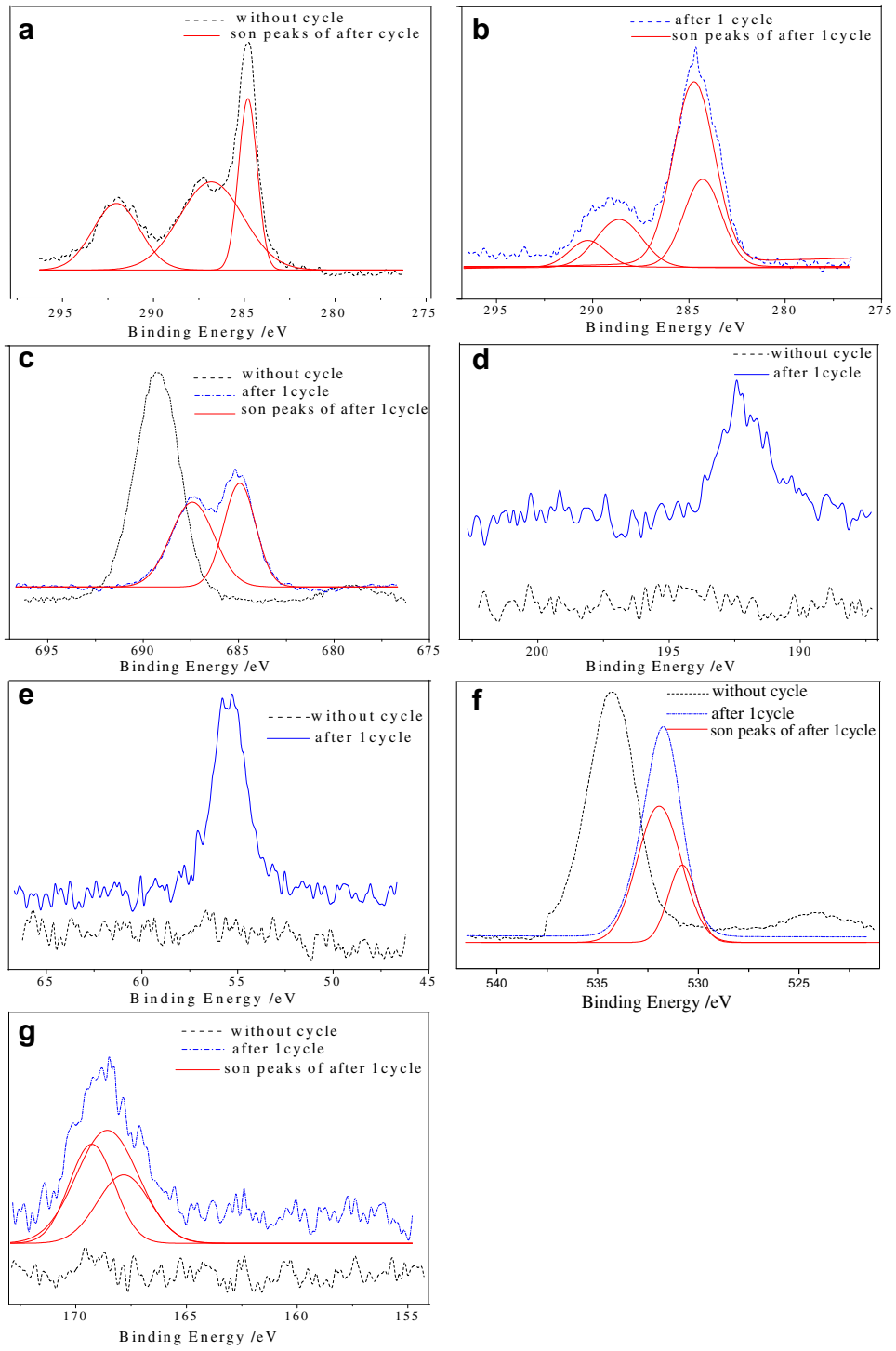

Fig. 4. XPS of different element on the surface of graphite anode before and after 1 cycle: a, C 1s peaks before cycle; b, C 1s peaks after cycle; c, F 1s; d, B 1s; e, Li 1s; f, O 1s; g, S 2p.

Generally, sulfurous compounds are better conductors of Li^+ ions than analogical carbonates, existences of these sulfurous compounds in SEI film are very helpful for impedance reduction [12,13].

4. Conclusion

Two kinds of electrolytes α and β are compared, and EIS impedances of cells with α electrolyte are lower than ones with β electrolyte. After 1 cycle a SEI film formed on surface of MCMB, and it becomes more and more smoothly along with the cycling procedure. After 10 cycles, the SEI film becomes pyknotic which helps transfer of Li^+ ions, but after 90 cycles, fissures emerge on the particle surface of MCMB, so stability of the SEI film was destroyed. Compositions of the SEI film with α electrolyte contain at least C_2H_5OLi, $C_2H_5CO_3Li$, Li_2CO_3, RSO_3Li, Li_2SO_3, LiF, C_2H_5F and some complicated mesh compounds based on >B—O— bond. It was believed that the root of impedance reduction benefits from both the rich existence of sulfurous compounds and the low content of

LiF in SEI film. Good film-forming property of both SL and LiODFB formation of a more conductive SEI film, LiODFB–EMC/SL electrolyte is an excellent candidate electrolyte for advanced lithium-ion batteries.

Acknowledgments

This work was supported by Science and Technology Planning Project of Gansu Province (No. 1107RJYA056), Branchy Tamarisk Development Program for Young Teachers of Lanzhou University of Technology (No.Q201105), and the Natural Science Foundation of China (No.20961004).

References

[1] J.M. Chen, C.Y. Yao, C.H. Cheng, W.M. Hurng, T.H. Kao, J. Power Sources 54 (1995) 494–495.
[2] K. Zaghib, K. Tatsumi, H. Abe, T. Ohsaki, Y. Sawada, S. Higuchi, J. Power Sources 54 (1995) 435–439.
[3] W.Q. Lu, Z.H. Chen, H. Joachin, J. Prakash, J. Liu, K. Amine, J. Power Sources 163 (2007) 1074–1079.
[4] K. Xu, S.S. Zhang, B.A. Poese, T.R. Jow, Electrochem. Solid State Lett. 5 (2002) A259–A262.
[5] K. Xu, S.S. Zhang, T.R. Jow, Electrochem. Solid State Lett. 6 (2003) A117–A120.
[6] K. Xu, U. Lee, S.S. Zhang, M. Wood, T.R. Jow, Electrochem. Solid State Lett. 6 (2003) A144–A148.
[7] G.V. Zhuang, K. Xu, T.R. Jow, P.N.J. Ross, Electrochem. Solid State Lett. 7 (2004) A224–A227.
[8] S.S. Zhang, Electrochem. Commun. 8 (2006) 1423–1428.
[9] S.S. Zhang, J. Power Sources 163 (2007) 713–718.
[10] C.R. Yang, Y.Y. Wang, C.C. Wan, J. Power Sources 72 (1998) 66–71.
[11] H. Nakahara, S. Nutt, J. Power Sources 160 (2006) 1355–1360.
[12] S.Y. Li, Y.Y. Zhao, X.M. Shi, B.C. Li, X.L. Xu, W. Zhao, X.L. Cui, Electrochim. Acta 65 (2012) 221–227.
[13] S.Y. Li, B.C. Li, X.L. Xu, X.M. Shi, Y.Y. Zhao, L.P. Mao, X.L. Cui, J. Power Sources 209 (2012) 295–300.
[14] E. Peled, D. Golodnitsky, C. Menachem, D. Bar-Tow, J. Electrochem. Soc. 145 (1998) 3482–3486.
[15] S. Santeea, X. Ang, Y.G. Li, J. Gnanaraj, B.L. Luchta, J. Power Sources 194 (2009) 1053–1060.
[16] D. Bar-Tow, E. Peled, L. Bursteinb, J. Electrochem. Soc. 146 (1999) 824–832.
[17] K. Xu, S.S. Zhang, U. Lee, J.L. Allen, T.R. Jow, J. Power Sources 146 (2005) 79–85.
[18] H. Kaneko, K. Sekine, T. Takamura, J. Power Sources 146 (2005) 142–145.
[19] K. Xu, S.S. Zhang, R. Jow, J. Power Sources 143 (2005) 197–202.
[20] E. Peled, D.B. Tow, A. Merson, A. Gladkich, L. Burstein, D. Golodnitsky, J. Power Sources 97–98 (2001) 52–57.